Study of the Temperature-Programmed Reaction Synthesis of Early Transition Metal Carbide and Nitride Catalyst Materials from Oxide Precursors

John B. Claridge,† Andrew P. E. York, Attila J. Brungs, and Malcolm L. H. Green*

Wolfson Catalysis Centre, Inorganic Chemistry Laboratory, University of Oxford, South Parks Road, Oxford OX1 3QR, U.K.

Received July 19, 1999. Revised Manuscript Received October 19, 1999

The synthesis of high surface area carbide and nitride materials from binary and ternary oxides of vanadium, niobium, tantalum, molybdenum, and tungsten, suitable for use as catalysts for a wide range of reactions, has been investigated via the temperature-programmed reaction (TPRe) method, in various gas mixtures. TPRe of oxides in CH_4/H_2, C_2H_6/H_2, or NH_3 yield materials with surface areas >40 $m^2\ g^{-1}$. For the reaction with ethane or ammonia the reaction appears to proceed topotactically while that with methane does not; however, the conversion of nitrides to carbides in CH_4/H_2 does appear to proceed topotactically.

Introduction

Transition metal carbides and nitrides are of great technological interest with many and varied applications,[1] e.g. as hard coatings and in machine tools,[2] golf shoe spikes, and snow tires. There has also been much interest in their electronic and magnetic properties.[3]

In the 1960s and 1970s, it was found that tungsten carbide showed catalytic properties similar to those of the noble metals.[4−7] This led to similar observations being made for other early transition metal carbides and transition metal nitrides.[8] However most of these studies were carried out on low surface area materials. The key to producing successful catalysts lies in the ability to synthesize materials of high surface area.[1,9]

It is the more recent development of high surface area systems that has led to an explosion of interest in the use of transition metal carbides and nitrides as catalysts, especially over the past decade. Thus, carbides and nitrides have been explored for a wide range of reactions. They have been shown to be particularly active for hydrotreating, especially hydrodenitrogenation (HDN),[10−21] hydrogenation reactions,[22−29] the Fischer−Tropsch reaction,[25,28,30−33] hydrocarbon isomerization,[29,34−37] and the oxyforming of methane.[38−40]

Some of the methods developed for synthesizing high surface area carbides and nitrides include gas-phase reactions of metal compounds,[41−43] reaction of gaseous reagents with solid-state metal compounds,[1,9,44] pyroly-

* To whom correspondence should be addressed. Telephone: +44-1865-272649. Fax: +44-1865-272690. E-mail: malcolm.green@chem.ox.ac.uk.

† Current address: Department of Chemistry, The University of Liverpool, Crown Street, Liverpool L69 7ZD, U.K.

(1) Oyama, S. T. *The Chemistry of Transition Metal Carbides and Nitrides*; Oyama, S. T., Ed.; Blackie Academic & Professional: Glasgow, Scotland, 1996; pp 1−27.
(2) Santhanam, A. T. *The Chemistry of Transition Metal Carbides and Nitrides*; Oyama, S. T., Ed.; Blackie Academic & Professional: Glasgow, 1996; pp 28−52.
(3) Toth, L. E. *Transition Metal Carbides and Nitrides*; Academic Press: New York, 1971; Vol. 7.
(4) Gaziev, G. A.; Krylov, O. V.; Roginskii, S. Z.; Samsonov, G. V.; Fokina, E. A.; Yanovskii, M. I. *Dokl. Akad. Nauk S. S. S. R.* **1961**, *140*, 863.
(5) Muller, J.-M.; Gault, F. G. *Bull. Soc. Chim. Fr.* **1970**, *2*, 416.
(6) Sinfelt, J. H.; Yates, D. J. C. *Nature Phys. Sci.* **1971**, *229*, 27.
(7) Levy, R. B.; Boudart, M. *Science* **1973**, *181*, 547.
(8) Oyama, S. T.; Haller, G. L. *Catalysis* **1982**, *3*, 333.
(9) Chorley, R. W.; Lednor, P. W. *Adv. Mater.* **1991**, *3*, 474.
(10) Abe, H.; Cheung, T.-K.; Bell, A. T. *Catal. Lett.* **1993**, *21*, 11.
(11) Choi, J.-G.; Brenner, J. R.; Colling, C. W.; Demczyk, B. G.; Dunning, J. L.; Thompson, L. T. *Catal. Today* **1992**, *15*, 201.
(12) Colling, C. W.; Thompson, L. T. *J. Catal.* **1994**, *146*, 193.
(13) Lee, J. S.; Boudart, M. *Appl. Catal.* **1985**, *19*, 207.
(14) Markel, E. J.; Van Zee, J. W. *J. Catal.* **1990**, *126*, 643.
(15) Nagai, M.; Miyao, T. *Catal. Lett.* **1992**, *15*, 105.
(16) Nagai, M.; Miyao, T.; Tuboi, T. *Catal. Lett.* **1993**, *18*, 9.
(17) Schlatter, J. C.; Oyama, S. T.; Metcalfe, J. E., III.; Lambert, J. M., Jr. *Ind. Eng. Chem. Res.* **1988**, *27*, 1648.
(18) Abe, H.; Bell, A. T. *Catal. Lett.* **1993**, *18*, 1.
(19) Lee, K. S.; Abe, H.; Reimer, J. A.; Bell, A. T. *J. Catal.* **1993**, *139*, 34.
(20) Choi, J.-G.; Brenner, J. R.; Thompson, L. T. *J. Catal.* **1995**, *154*, 33.
(21) Yu, C. C.; Ramanathan, S.; Sherif, F.; Oyama, S. T. *J. Phys. Chem.* **1994**, *98*, 13038.
(22) Kojima, I.; Miyazaki, E.; Inoue, Y.; Yasumori, I. *J. Catal.* **1982**, *73*, 128.
(23) Leclercq, L.; Provost, M.; Pastor, H.; Leclerq, G. *J. Catal.* **1989**, *117*, 384.
(24) Lee, J. S.; Yeom, M. H.; Park, K. Y.; Nam, I.-S.; Chung, J. S.; Kim, Y. G.; Moon, S. H. *J. Catal.* **1991**, *128*, 126.
(25) Ranhotra, G. S.; Bell, A. T.; Reimer, J. A. *J. Catal.* **1987**, *108*, 40.
(26) Vidick, B.; Lemaitre, J.; Leclerq, L. *J. Catal.* **1986**, *99*, 439.
(27) Abe, H.; Bell, A. T. *J. Catal.* **1993**, *142*, 430.
(28) Djéga-Mariadassou, G.; Boudart, M.; Bugli, G.; Sayag, C. *Catal. Lett.* **1995**, *31*, 411.
(29) Sherif, F.; Vreugdenhil, W. *The Chemistry of Transition Metal Carbides and Nitrides*; Oyama, S. T., Ed.; Blackie Academic & Professional: Glasgow, Scotland, 1996; pp 414−425.
(30) Park, K. Y.; Seo, W. K.; Lee, J. S. *Catal. Lett.* **1991**, *11*, 349.
(31) Liu, J.; Shen, J.; Gao, X.; Lin, L. *J. Therm. Anal.* **1993**, *40*, 1239.
(32) Dubois, J.-L.; Sayama, K.; Arakawa, H. *Chem. Lett.* **1992**, 5.
(33) Leclercq, L.; Almazouari, A.; Dufour, M.; Leclercq, G. *The Chemistry of Transition Metal Carbides and Nitrides*; Oyama, S. T., Ed.; Blackie Academic & Professional: Glasgow, Scotland, 1996; pp 345−361.
(34) Pham-Huu, C.; York, A. P. E.; Benaissa, M.; Del Gallo, P.; Ledoux, M. J. *Ind. Eng. Chem. Res.* **1995**, *34*, 1107.
(35) Keller, V.; Weher, P.; Garin, F.; Ducros, R.; Maire, G. *J. Catal.* **1995**, *153*, 9.

10.1021/cm9911060 CCC: $19.00
Published on Web 12/15/1999

sis of metal precursors[45] and solution reactions.[46,47] Among these, one of the most promising and widely used is the temperature-programmed method (TPRe) developed by Boudart and co-workers.[48−50] Nearly all the work to date has concentrated on the synthesis of carbides and nitrides of molybdenum and tungsten, with the exception of iron catalysts for Fischer−Tropsch chemistry, with very little work being done on the other metals,[17,18,51−57] and even less on mixed metal systems,[21,58−62] despite the promise shown by these systems. Therefore, the TPRe method of synthesis has been further investigated for the synthesis of binary and ternary early transition metal carbides suitable for catalytic applications.

Experimental Section

The apparatus used in this work was an upgraded version of the commercial Labcon microreactor, which has been described previously.[63,64] Ammonia was immediately vented, due to its corrosive nature, to avoid damage to the mass selective detector. Masses 10−50 were scanned, with gases CO, CO_2, H_2O, CH_4, and N_2 all monitored by their mass ions. In the case of N_2 the signal was adjusted to take into account thermal reactions of methane by deducting the signal of 27 amu. A 100 mg sample of the oxide was used in all cases. Samples for BET and XRD were heated at a rate of 1 K min^{-1} to the final temperature which was held for 90 min. After reaction, the samples were quenched to room temperature under argon by removing the tube from the furnace. Before exposure to the atmosphere, the samples were passivated in flowing 1 vol % O_2/Ar. The surface areas of the materials were then determined by the BET method.

Methane (Union Carbide, >99.95%), ethane (BOC, CP grade), ammonia (BOC, CP grade), hydrogen (BOC, CP grade), argon (BOC, CP grade), and oxygen (BOC, CP grade) were used as received without further purification. MoO_3 (Johnson Matthey, Puratronic 99.998%), WO_3 (Johnson Matthey, Puratronic 99.998%), Ta_2O_5 (Johnson Matthey, Puratronic 99.998%), and V_2O_5 (Johnson Matthey, Puratronic 99.995%) were used as supplied. Other oxides were synthesized as follows: H−Nb_2O_5, $WNb_{12}O_{33}$, $W_3Nb_{14}O_{44}$, and $W_9Nb_8O_{47}$ were prepared via the method described by Tilley and co-workers,[65] by crushing together appropriate quantities of WO_3 powder and Nb_2O_5 powder (Johnson Matthey, 99.9985%) in an agate pestle and mortar. The material was then formed into pellets and fired in a platinum crucible at 973 K for 10 days followed by 1473 K for 4 days. The pellets were crushed to a fine powder prior to use. XRD powder diffraction matched those quoted by Roth.[66] $MoNb_{12}O_{33}$, $Mo_3Nb_{14}O_{44}$, $Mo_3Nb_2O_{14}$, and $Mo_2Ta_2O_{11}$ were prepared via the method described by Ekstrom and co-workers[67] ($Mo_2Ta_2O_{11}$ is the phase they erroneously call $Ta_2O_5 \cdot 3MoO_3$), by crushing together appropriate quantities of MoO_3, Nb_2O_5, and Ta_2O_5 powder in an agate pestle and mortar. The material was then formed into pellets, crushed again, and fired in a sealed silica ampule at 1170 K for 15 days. The resultant powder was crushed prior to use. XRD powder diffraction data matched those quoted in JPDS. XRD of the starting materials are shown in Figure 1. All starting materials had BET surface areas less than 3 m^2 g^{-1}. High-resolution analytical electron microscopy was carried out using a JEOL-2000FX instrument with a Tracor Northern TN5500 energy-dispersive X-ray detector, and a JEOL-4000FX.

Results

Three methods for the preparation of carbides and one method for the preparation of nitrides are described. The synthesis, surface areas, and particle sizes for each method will be discussed below, while the morphology and possible topotactic nature of the reactions will be discussed later.

Methane Carburization of Oxides. TPRe was carried out using a flow of 250 cm^3 min^{-1} of 20 vol % CH_4/H_2 over V_2O_5, H−Nb_2O_5, L-Ta_2O_5, $W_9Nb_8O_{47}$, $Mo_3Nb_2O_{14}$, and $Mo_2Ta_2O_{11}$ at a heating rate of 10 K min^{-1}, which previous studies have shown to be suitable for carbide formation.[48,49,68] Temperatures were chosen based on studies by Oyama and co-workers,[69,70] where it was shown that Nb_2O_5 could be converted into NbC at 1170 K, which was recently confirmed by Djéga-Mariadassou and co-workers.[57] To compare the reactivity of the binary and ternary systems, this was taken as the standard temperature for all niobium-containing samples. Vanadium oxide has also been reported to

(36) Lee, J. S.; Song, B. J.; Li, S.; Woo, H. C. *The Chemistry of Transition Metal Carbides and Nitrides*; Oyama, S. T., Ed.; Blackie Academic & Professional: Glasgow, Scotland, 1996; pp 398−413.
(37) Ledoux, M. J.; Pham-Huu, C.; York, A. P. E.; Blekkan, E. A.; Delporte, P.; Del Gallo, P. *The Chemistry of Transition Metal Carbides and Nitrides*; Oyama, S. T., Ed.; Blackie Academic & Professional: Glasgow, 1996; pp 373−397.
(38) York, A. P. E.; Claridge, J. B.; Brungs, A. J.; Tsang, S. C.; Green, M. L. H. *Chem. Commun.* **1997**, 39.
(39) York, A. P. E.; Claridge, J. B.; Márquez-Alvarez, C.; Brungs, A. J.; Tsang, S. C.; Green, M. L. H. *Stud. Surf. Sci. Catal.* **1997**, *110*, 711.
(40) Claridge, J. B.; York, A. P. E.; Brungs, A. J.; Márquez-Alvarez, C.; Sloan, J.; Tsang, S. C.; Green, M. L. H. *J. Catal.* **1998**, *180*, 85.
(41) O'Brien, R. J.; Xu, L.; Bi, X. X.; Eklund, P. C.; Davis, B. H. *The Chemistry of Transition Metal Carbides and Nitrides*; Oyama, S. T., Ed.; Blackie Academic & Professional: Glasgow, Scotland, 1996; pp 362−372.
(42) Ledoux, M. J.; Pham-Huu, C. *Catal. Today* **1992**, *15*, 263.
(43) Ledoux, M. J.; Hantzer, S.; Pham-Huu, C.; Guille, J.; Desaneaux, M.-P. *J. Catal.* **1988**, *114*, 176.
(44) Leclercq, L.; Provost, M.; Pastor, H.; Grimblot, J.; Hardy, A. M.; Gengembre, L.; Leclercq, G. *J. Catal.* **1989**, *117*, 371.
(45) Giraudon, J.-M.; Leclercq, L.; Leclercq, G.; Lofberg, A.; Frennet, A. *J. Mater. Sci.* **1993**, *28*, 2449.
(46) Zeng, D.; Hampden-Smith, M. J. *Chem. Mater.* **1993**, *5*, 681.
(47) Zeng, D.; Hampden-Smith, M. J. *Chem. Mater.* **1992**, *4*, 968.
(48) Volpe, L.; Boudart, M. *J. Solid State Chem.* **1985**, *59*, 348.
(49) Volpe, L.; Boudart, M. *J. Solid State Chem.* **1985**, *59*, 332.
(50) Wrobleski, J. T.; Boudart, M. *Catal. Today* **1992**, *15*, 349.
(51) Chen, J. G. *J. Catal.* **1995**, *154*, 80.
(52) Chen, J. C.; Fruhberger, B.; Weisel, M. D.; Baumgartner, J. E.; De Vries, B. D. *The Chemistry of Transition Metal Carbides and Nitrides*; Oyama, S. T., Ed.; Blackie Academic & Professional: Glasgow, Scotland, 1996; pp 439−454.
(53) Choi, J. G.; Jung, M. K.; Choi, S.; Park, T. K.; Kuk, I. H.; Yoo, J. H.; Park, H. S.; Lee, H. S.; Ahn, D. H.; Chung, H. S. *Bull. Chem. Soc. Jpn.* **1997**, *70*, 993.
(54) Meunier, F.; Delporte, P.; Heinrich, B.; Bouchy, C.; Crouzet, C.; Pham-Huu, C.; Panissod, P.; Lerou, J. J.; Mills, P. L.; Ledoux, M. J. *J. Catal.* **1997**, *169*, 33.
(55) Schwartz, V.; Oyama, S. T. *Chem. Mater.* **1997**, *9*, 3052.
(56) Choi, J. G.; Oh, H. G.; Baek, Y. S. *J. Ind. Eng. Chem.* **1998**, *4*, 94.
(57) Kim, H. S.; Bugli, G.; Djéga-Mariadassou, G. *J. Solid State Chem.* **1999**, *142*, 100.
(58) Yu, C. C.; Oyama, S. T. *J. Solid State Chem.* **1995**, *116*, 205.
(59) Kapoor, R.; Oyama, S. T.; Fruhberger, B.; Chen, J. G. *J. Phys. Chem. B* **1997**, *101*, 1543.
(60) Ramanathan, S.; Yu, C. C.; Oyama, S. T. *J. Catal.* **1998**, *173*, 1.
(61) Ramanathan, S.; Yu, C. C.; Oyama, S. T. *J. Catal.* **1998**, *173*, 10.
(62) Zhang, Y.; Li, Y.; Raval, R.; Li, C.; Zhai, R.; Xin, Q. *J. Mol. Catal. A−Chem.* **1998**, *132*, 241.
(63) Claridge, J. B.; Green, M. L. H.; Tsang, S. C.; York, A. P. E. *Appl. Catal. A: Gen.* **1992**, *89*, 103.
(64) Claridge, J. B.; Green, M. L. H.; Tsang, S. C.; York, A. P. E. *J. Chem. Soc., Faraday Trans.* **1993**, *89*, 1089.
(65) Viccary, M. W.; Tilley, R. J. D. *J. Solid State Chem.* **1993**, *104*, 131.
(66) Roth, R. S.; Waring, J. L. *J. Res. Natl. Bur. Stand.−A. Phys. Chem.* **1966**, *70*, 281.
(67) Ekstrom, T. *Acta Chem. Scand.* **1971**, *25*, 2591.
(68) Lee, J. S.; Oyama, S. T.; Boudart, M. *J. Catal.* **1987**, *106*, 125.
(69) Teixeira da Silva, V. L. S.; Ko, E. I.; Schmal, M.; Oyama, S. T. *Chem. Mater.* **1995**, *7*, 179.
(70) Teixeira da Silva, V. L. S.; Schmal, M.; Oyama, S. T. *J. Solid State Chem.* **1996**, *123*, 168.

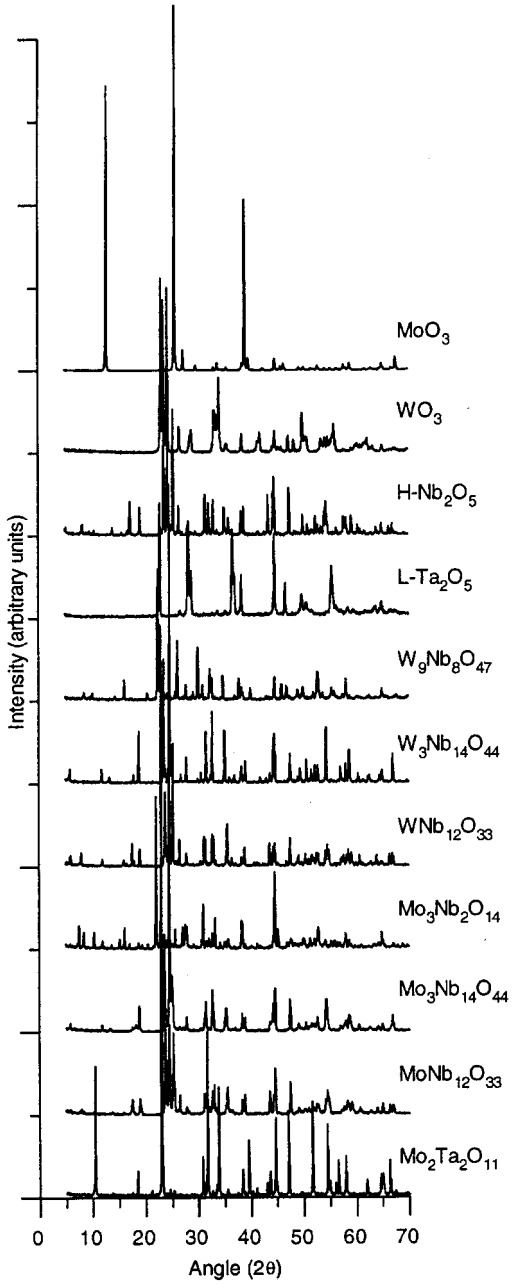

Figure 1. XRD of the oxide starting materials.

react in this temperature range,[71] and therefore the same conditions were used for V_2O_5. For L-Ta_2O_5, it was found that very little reaction took place at 1170 K while TaC was formed if the final temperature was raised to 1220 K, which is consistent with a recent report of the synthesis of TaC.[56] This final temperature was also used for $Mo_2Ta_2O_{11}$. TPRe plots for the oxides are shown in Figure 2; only the traces for CO and H_2O are shown as in all cases CO_2 gave very weak signals mirroring CO peaks, while the high background meant that the CH_4 trace was rather featureless.

Vanadium shows peaks in the water trace at 840 and 865 K, and a much smaller broad peak around 1170 K, while the main peak for carbon monoxide is centered at ~1170 K, with two smaller peaks at 790 and 830 K; this is broadly similar to the behavior reported by

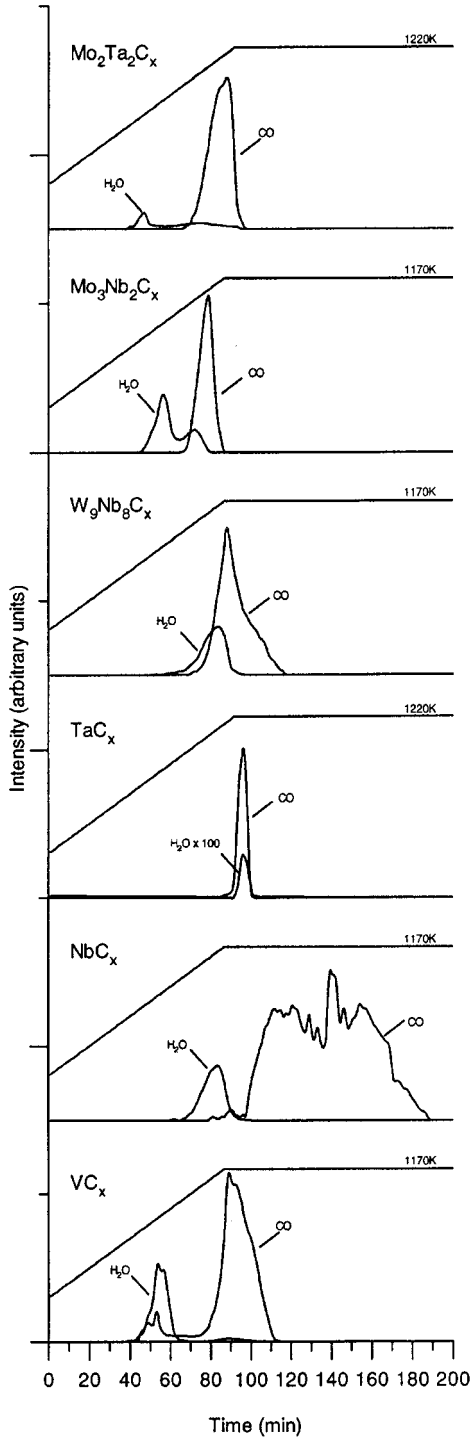

Figure 2. Methane TPRe of the precursor oxides (20% CH_4/H_2, 300 K − T_f, 10 K min^{-1}).

Kapoor and Oyama,[71] indicating the initial formation of V_2O_3. The trace for niobium oxide is again similar to that reported by Oyama and co-workers,[69] with a water peak at 1130 K and a complex carbon monoxide feature during the time at constant temperature. The tantalum oxide trace has two interesting features: first very little water is formed during the reduction and, second, only one reduction peak at ~1220 K is observed. In the case of niobium and vanadium the presence of a lower temperature peak was associated with the formation of an intermediate oxide phase. This does not appear to occur for tantalum. XRD of the partially reacted samples showed no sign of phases other than L-Ta_2O_5 and TaC.

(71) Kapoor, R.; Oyama, S. T. *J. Solid State Chem.* **1992**, *99*, 303.

Table 1. Comparison of Particle Sizes Derived from XRD and BET Isotherms for Carbides Synthesized from the Oxides with CH_4 as Carburizing Agent

material	a_0 (nm)	$r_{(220)}{}^a$ (nm)	S_g ($m^2\,g^{-1}$)	$r_{(BET)}{}^b$ (nm)
VC_x	0.4137	15.5	44	23.6
NbC_x	0.4469	14.7	62	12.4
TaC_x	0.4449	9.7	54	8.0
$W_9Nb_8C_x$	ND	ND	88	4.4
$Mo_3Nb_2C_x$	0.4335	6.8	80	8.7
$Mo_2Ta_2C_x$	0.4379	4.4	52	10.0

[a] $D_c = 0.9\lambda/(\beta \cos \theta)$. [b] $D_\rho = 6/(\rho S_g)$.

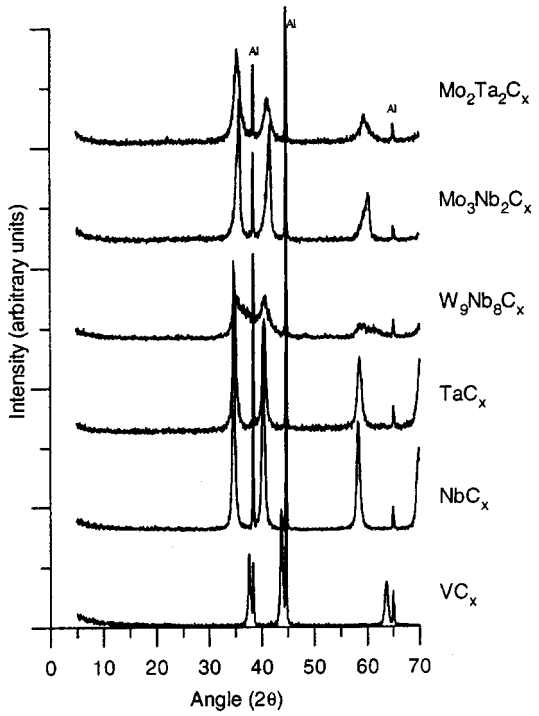

Figure 3. XRD patterns of the materials formed by the methane TPRe of oxides.

In the case of the ternary oxides of group V and VI, the formation of the carbide seems to proceed more readily with carbon consuming reactions occurring either more rapidly or at lower temperature. This effect is most marked for $Mo_3Nb_2O_{14}$, where there are water peaks at 870 and 1090 K and a carbon monoxide peak at 1125 K. For $Mo_2Ta_2O_{11}$, there is a water peak at 770 K and a small broad peak at 1120 K with the carbon monoxide peak shifted to 1180 K. $W_9Nb_8O_{47}$ is least affected, relative to the binary group V oxide, with water and carbon monoxide peaks at 1140 K and ~1170 K respectively, though the reaction is finished in 120 min as opposed to 190 min for H−Nb_2O_5. Thus, in all cases the group VI component participated in some way in the reaction, resulting in lower reduction temperatures.

Table 1 and Figure 3 show the XRD data for the materials after TPRe. Table 1 also shows the BET surface areas of the samples after passivation. In all cases, except $W_9Nb_8O_{47}$, the product was a single phase cubic material; for $W_9Nb_8O_{47}$, the product phase was unclear. However, in the case of $Mo_2Ta_2O_{11}$, the peaks associated with the carbide were highly asymmetric. In no case was evidence for the presence of the hexagonal carbides, α-WC or β-Mo_2C, found by XRD or HRTEM. For the binary oxides the obtained values of a_0 were close to those given in the literature for the carbides[72]

Table 2. Summary of XRD Data and BET Surface Areas for the Nitrides

material	a_0 (nm)	$r_{(220)}{}^a$ (nm)	S_g ($m^2\,g^{-1}$)	$r_{(BET)}{}^b$ (nm)
VN_x (1073 K)	0.4129	13.3	51	19.2
NbN_x (1073 K)	0.4322	9.8	69	10.4
NbN_x (973 K)	0.4308	8.9	82	8.7
$WNb_{12}N_x$ (1073 K)	0.4312	9.5	67	10.3
$W_3Nb_{14}N_x$ (1073 K)	0.4317	9.4	65	9.5
$W_9Nb_8N_x$ (1073 K)	0.4257	6.3	107	4.6
$MoNb_{12}N_x$ (1073 K)	0.4328	10.7	64	11.3
$Mo_3Nb_{14}N_x$ (1073 K)	0.4311	7.4	101	7.0
$Mo_3Nb_2N_x$ (1073 K)	0.4239	4.2	142	4.8
$Mo_2Ta_2N_x$ (1123 K)	0.4250	4.6	59	8.0

[a] $D_c = 0.9\lambda/(\beta \cos \theta)$. [b] $D_\rho = 6/(\rho S_g)$.

($VC_{0.73-0.97}$, a_0 = 4.1310−4.1655 Å; $NbC_{0.70-0.99}$, a_0 = 4.4318−4.4707 Å; and $TaC_{0.70-0.99}$, a_0 = 4.4100−4.4555 Å). As can be seen, the TPRe reaction gave materials with high surface areas.

Ammonia Nitridation of Oxides. TPRe was carried out at a heating rate of 1 K min^{-1} in a flow of 100 cm^3 min^{-1} of ammonia over V_2O_5, H−Nb_2O_5, L-Ta_2O_5, $WNb_{12}O_{33}$, $W_3Nb_{14}O_{44}$, $W_9Nb_8O_{47}$, $MoNb_{12}O_{33}$, $Mo_3Nb_{14}O_{44}$, $Mo_3Nb_2O_{14}$, $MoTa_{12}O_{33}$, and $Mo_2Ta_2O_{11}$. Final temperatures were held for 3 h in line with previous studies.[20,48,49,68,73] Due to the corrosive nature of ammonia, the reaction products were not monitored, and the end points of the synthesis were obtained by attempting the reaction at increasing final temperatures until a pure nitride phase was achieved. The results for the nitrides are summarized in Table 2.

The temperatures used for vanadium[53,71,74] and niobium[55,75] were taken from previous studies; the surface areas obtained are close to those reported in the literature. The synthesis of Ta_3N_5 from Ta_2O_5 has been previously reported under isothermal conditions[76,77] at 1170 K. Figure 4 shows the XRD of the products of ammonia TPRe of L-Ta_2O_5 at various temperatures (the final product at 1070 K had a surface area of 72 $m^2\,g^{-1}$). In contrast to the work of Grins et al.,[76] no formation of the baddeleyite tantalum oxynitride, TaON, was observed and Ta_3N_5 was the only phase present at 1073 K. This first is probably due to the fact that Grins et al. treated their samples for ~ 96 h at the final temperature, indicating that TaON forms only slowly, and that it is therefore unlikely to be an intermediate in the formation of Ta_3N_5, while the difference in final temperature is probably due to different extents of ammonia decomposition vide infra. Despite the numerous reports on the synthesis of ternary nitrides from oxides,[76,78−84] very little work has been done on the synthesis of high

(72) Storms, E. K. *The Refractory Carbides*; Academic Press: New York, 1967; Vol. 2.
(73) Choi, J.-G.; Curl, R. L.; Thompson, L. T. *J. Catal.* **1994**, *146*, 218.
(74) Oyama, S. T.; Kapoor, R.; Oyama, H. T.; Hofmann, D. J.; Matijevic, E. *J. Mater. Res.* **1993**, *8*, 1450.
(75) Kim, H. S.; Shin, C. H.; Bugli, G.; Bureau-Tardy, M.; Djéga-Mariadassou, G. *Appl. Catal. A: Gen.* **1994**, *119*, 223.
(76) Grins, J.; Kall, P.-O.; Svensson, G. *J. Mater. Chem.* **1994**, *4*, 1293.
(77) Elder, S. H.; DiSalvo, F. J.; Topor, L.; Navrotsky, A. *Chem. Mater.* **1993**, *5*, 1545.
(78) Bacher, P.; Antoine, P.; Marchand, P.; L'Haridon, P.; Laurent, Y.; Roult, G. *J. Solid State Chem.* **1988**, *77*, 67.
(79) Bem, D. S.; zur Loye, H.-K. *J. Solid State Chem.* **1993**, *104*, 467.
(80) Bem, D. S.; Gibson, C. P.; zur Loye, H.-C. *Chem. Mater.* **1993**, *5*, 397.

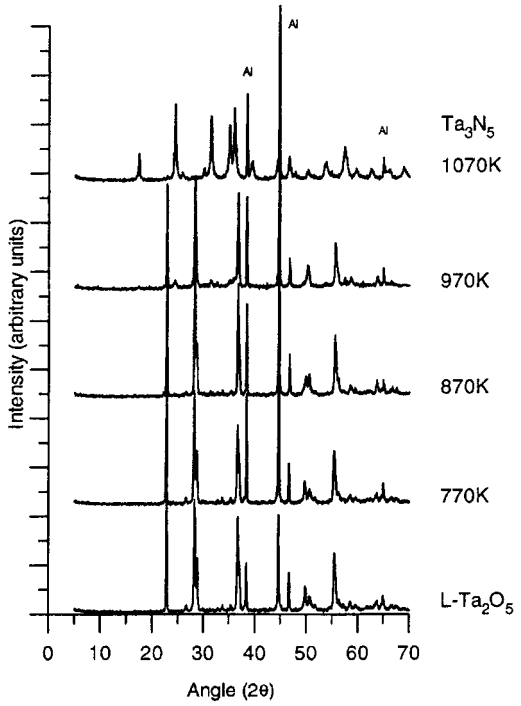

Figure 4. XRD patterns of L-Ta_2O_5 nitrided at intermediate temperatures under flowing ammonia, during the synthesis of Ta_3N_5.

surface area nitride materials.[58] In contrast to the work on the carburization of ternary oxides, it was found that, in the case of the nitrides, the final temperatures required were higher than for the binary oxides. In the case of niobium based ternary systems, temperatures of 1070 K were required, while for $Mo_2Ta_2O_{11}$, 1120 K was needed to obtain only the nitride. This observation is in agreement with those of Yu and Oyama[58] for $2V_2O_5{\cdot}MoO_3$, $Nb_2O_5{\cdot}3MoO_3$, $V_2O_5{\cdot}2WO_3$, $WO_3{\cdot}MoO_3$, and $Nb_2O_5{\cdot}3WO_3$. However, for $MoTa_{12}O_{33}$, the material was still largely unconverted at all temperatures, even with prolonged heating (>48 h) at temperatures up to 1220 K.

Figure 5 shows the XRD patterns of the synthesized nitrides. With the exception of Ta_3N_5, all the products have rock salt type fcc structures. Lattice parameters and particle sizes derived from the Scherrer equation are listed in Table 2. In all cases, except $Mo_2Ta_2O_{11}$, the particle sizes from XRD and BET were in agreement, indicating that the particles are single crystallites as opposed to agglomerates. For $Mo_2Ta_2O_{11}$, the particle size from XRD is about half that for BET, indicating that other sources of broadening are present; this is probably due to defects or disorder in the nitride.

Methane Carburization of Nitrides. Volpe and Boudart[48] demonstrated that Mo_2N and W_2N could be converted into the carbides by TPRe in CH_4/H_2 mixtures while retaining the surface area and orientation of the parent nitride; however, this has not been extended to other systems. The carburization of the nitride materials

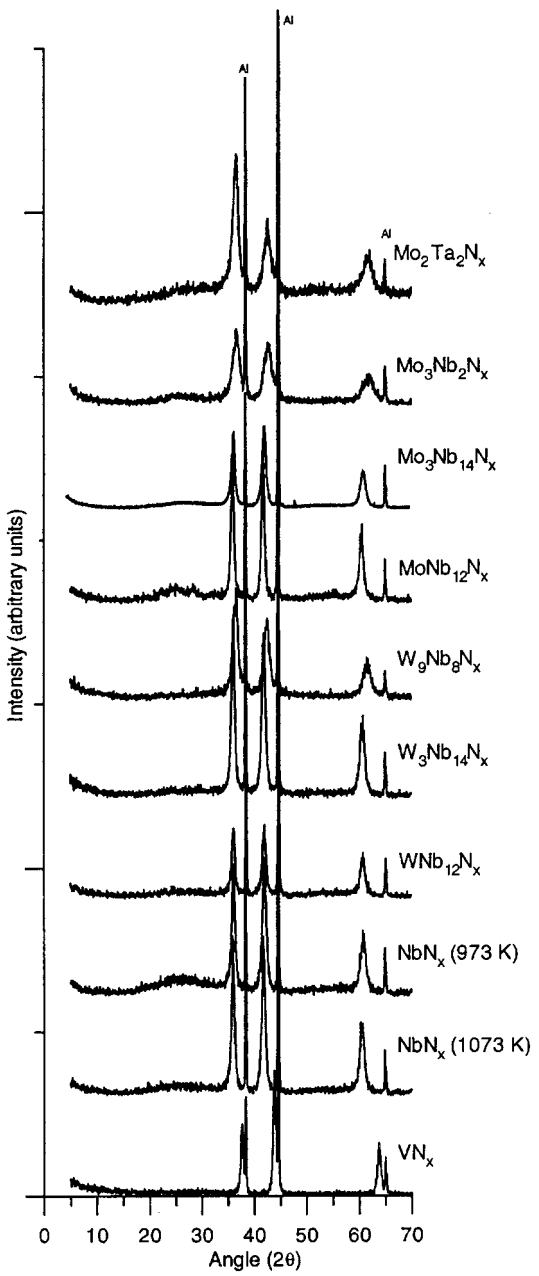

Figure 5. XRD patterns for the cubic phases formed by nitriding oxides.

formed above was thus investigated for those derived from V_2O_5, H−Nb_2O_5, L-Ta_2O_5, $W_9Nb_8O_{47}$, $Mo_3Nb_2O_{14}$, and $Mo_2Ta_2O_{11}$. TPRe was performed in a flow of 250 $cm^3\ min^{-1}$ of 20 vol % CH_4/H_2 and at a heating rate of 5 K min^{-1} to a maximum temperature of 1170 K (which was sufficient to convert all materials). N_2 evolution is shown in Figure 6.

Vanadium nitride gives two nitrogen evolution peaks, with the first major peak at 950 K and a minor peak at 1120 K. For niobium there is a dinitrogen peak at 1125 K with a shoulder at 1155 K. Tantalum shows only one feature, which peaks during the dwell at 1170 K. It should be noted that this order of reactivity is mirrored in the ability of the metals to form nitrides; i.e., the most nitrogen-rich nitrides formed are in the order $VN_{1.0}$, Nb_3N_4, and Ta_3N_5.[85] As was the case with the direct reaction of the oxides, the presence of group VI metals in the ternary systems substantially reduces the tem-

(81) Elder, S. H.; Doerrer, L. H.; DiSalvio, F. J.; Praise, J. B.; Guyomard, D.; Tarascon, J. M. *Chem. Mater.* **1992**, *4*, 928.
(82) Grins, J.; Kall, P.-O.; Svensson, G. *J. Solid State Chem.* **1995**, *117*, 48.
(83) Grins, J.; Kall, P.-O.; Svensson, G. *J. Mater. Chem.* **1995**, *5*, 571.
(84) Marchand, R.; Pors, F.; Laurent, Y. *Ann. Chim. Fr.* **1991**, *16*, 553.

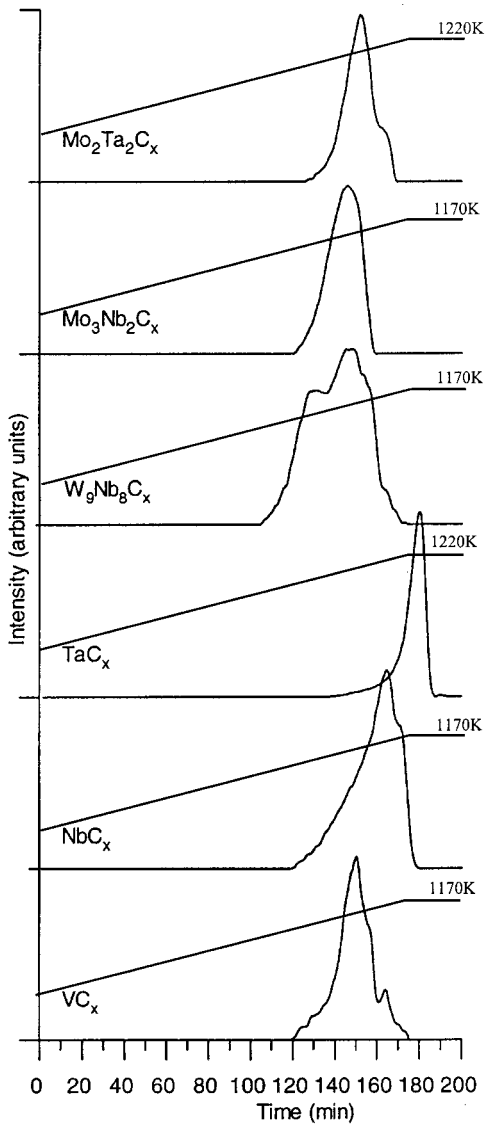

Figure 6. Methane TPRe of nitrides (20% CH_4/H_2, 300 K − T_f, 5 K min^{-1}).

Table 3. Comparison of Particle Sizes Derived from XRD and BET Isotherms for Carbides Synthesized from the Nitrides with CH_4 as the Carburizing Agent

material	a_0 (nm)	$r_{(220)}{}^a$ (nm)	S_g ($m^2\,g^{-1}$)	$r_{(BET)}{}^b$ (nm)
VC_x	0.4151	14.5	49	21.2
NbC_x	0.4465	9.7	76	10.1
TaC_x	0.4427	8.3	70	6.2
$W_9Nb_8C_x$	0.4396	6.5	107	4.7
$Mo_3Nb_2C_x$	0.4345	4.0	136	4.8
$Mo_2Ta_2C_x$	0.4384	5.4	55	9.5

^{a} $D_c = 0.9\lambda/\beta \cos\theta$). ^{b} $D_\rho = 6/(\rho S_g)$.

peratures required in order to fully carburize the nitride. Thus, $W_9Nb_8N_x$ gives two broad peaks at 960 and 1040 K, $Mo_3Nb_2N_x$ gives a single broad peak centered at 1030 K, and $Mo_2Ta_2N_x$ gives one peak at 1050 K with a shoulder at 1115 K.

Table 3 lists the BET surface areas and lattice parameters for the cubic carbide materials formed in the TPRe of the nitrides. The XRD patterns are also shown in Figure 7. Particle sizes and surface areas are similar to those obtained for the nitrides and the fcc

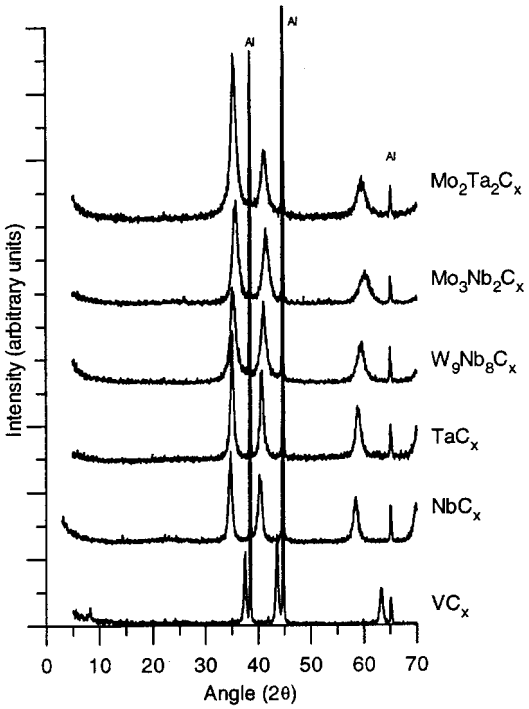

Figure 7. XRD patterns for the cubic phases formed by carburizing the nitrides.

structure of the nitride is maintained in all cases, although Ta_3N_5 also yields a cubic carbide. The lattice parameters for VC_x, NbC_x, and TaC_x are again close to those given in the literature for the carbides[72] ($VC_{0.73-0.97}$, $a_0 = 4.1310-4.1655$ Å; $NbC_{0.70-0.99}$, $a_0 = 4.4318-4.4707$ Å; and $TaC_{0.70-0.99}$, $a_0 = 4.4100-4.4555$ Å), while those of the ternary systems are similar to those for the TPRe of the oxides. The small differences may be due to residual nitrogen or oxygen in the lattice or different carbon contents due to the slightly different conditions employed in the synthesis. Therefore, it can be seen that the conversion of high surface area nitrides to carbides appears general for group V and VI systems.

Ethane Carburization of Oxides. Given the success of using nonequilibrium gas compositions for the nitridation of oxides and metals,[49,77,83,86-89] and the report by Frennet and co-workers[90] showing that for tungsten oxide, lower reduction temperatures and higher surface areas were obtained, the use of nonequilibrium gases containing C/H was investigated. To achieve this, 250 $cm^3\,min^{-1}$ of 1/8.6 C_2H_6/H_2 (H/C ratio identical to that used for methane TPRe) was passed over the oxides at a ramping rate of 1 K min^{-1}. Because of the decomposition of the C_2H_6 to CH_4 and C_2H_4, the TPRe are not very informative, though they do provide some indication of when the ethane starts to react, allowing an estimate of the final temperature required. The reactions of MoO_3, WO_3, V_2O_5, H−Nb_2O_5, L-Ta_2O_5, $W_9Nb_8O_{47}$, $Mo_3Nb_2O_{14}$, and $Mo_2Ta_2O_{11}$ were investigated. L-Ta_2O_5 did not react at any of the temperatures

(85) Brese, N. E.; O'Keeffe, M. *Struct. Bonding* **1992**, *79*, 307.
(86) Katsura, M. *J. Alloys Compd.* **1992**, *182*, 91.
(87) Katsura, M.; Hirota, M.; Nakagawa, T.; Miyake, M. *J. Alloys Compd.* **1994**, *207/208*, 413.
(88) Bamberger, C. E.; Allard, L. F.; Coffey, D. W.; Bennett, M. R. *J. Cryst. Growth* **1991**, *112*, 47.
(89) Oyama, S. T.; Schlatter, J. C.; Metcalfe, J. E., III.; Lambert, J. M., Jr. *Ind. Eng. Chem. Res.* **1988**, *27*, 1639.
(90) Decker, S.; Lofberg, A.; Bastin, J. M.; Frennet, A. *Catal. Lett.* **1997**, *44*, 229.

Table 4. Comparison of Particle Sizes Derived from XRD and BET Isotherms for Carbides Synthesized from the Oxides with C_2H_6 as Carburizing Agent

material	a_0 (nm)	$r_{(220)}{}^a$ (nm)	S_g ($m^2\ g^{-1}$)	$r_{(BET)}{}^b$ (nm)
β-Mo_2C[c]	0.302 (c_0 = 0.474 nm)[c]	4.9[c]	174	3.7
β-W_2C[c]	0.300 (c_0 = 0.473 nm)[c]	4.0[c]	71	5.4
VC_x	0.4152	13.1	76	13.7
NbC_x	0.4465	7.6	113	7.0
$W_9Nb_8C_x$	0.4359	2.7	102	8.2
$Mo_3Nb_2C_x$	0.4351	2.7	156	4.5
$Mo_2Ta_2C_x$	0.4351	1.9	84	6.2

[a] $D_c = 0.9\lambda/(\beta \cos\theta)$. [b] $D_\rho = 6/(\rho S_g)$. [c] Hexagonal carbides $r_{(11\bar{2}0)}$.

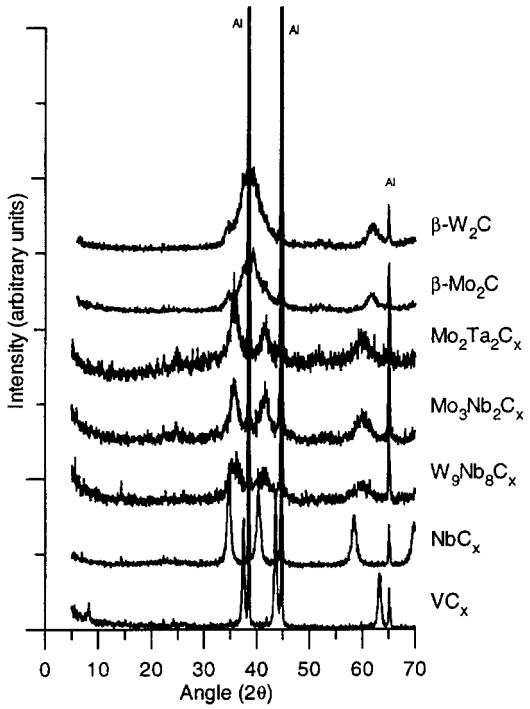

Figure 8. XRD patterns for the phases formed by carburizing oxides with ethane.

studied, with only the starting material present after reaction according to XRD. V_2O_5 and H-Nb_2O_5 required temperatures of 1020 K for complete reaction, and beneath this temperature V_2O_3 and NbO_2 were formed as detected by XRD. The remaining oxides gave carbide phases with no oxides present at 900 K. Therefore, as with methane, the mixed oxides of group V are much more reactive than the binaries.

Table 4 gives the XRD and BET data for the carbide materials formed using ethane; the XRD are shown in Figure 8. It can be seen that all the systems form fcc carbides, except molybdenum and tungsten which both form hcp carbides (in contrast to Frennet[90] where α-WC was observed). For the binary carbides the particle sizes derived from XRD and BET are in fair agreement. The ternary carbides are poorly crystalline with $r_{XRD} < r_{BET}$. Examination by XRD and HRTEM, however, shows the presence of only a single phase carbide, and no evidence of phase segregation or oxide phases was found.

Discussion

Thermodynamic Considerations/Equilibria. It has been shown that ammonia and ethane are very reactive for the conversion of early transition metal oxides. It is well-known that NH_3 and C_2H_6 are considerably more reactive than N_2 and CH_4, respectively. However, it should also be noted that nonequilibrium gas mixtures, which can be obtained by using flowing gases, can lead to very high driving forces for reactions. This can be most clearly seen if we consider the reaction of a metal with ammonia. There are three possible reactions:

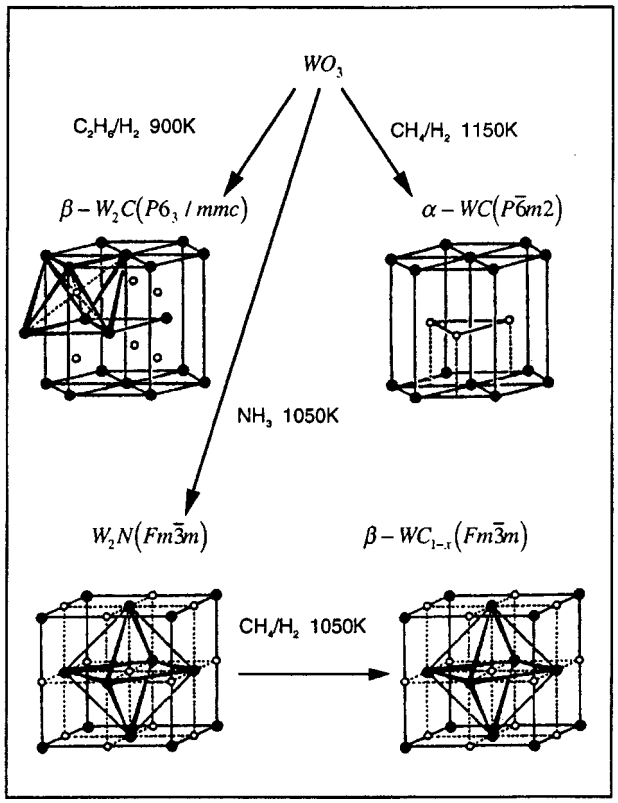

Figure 9. Routes to the various tungsten carbide phases via TPRe. (Note, for α-W_2C, W_2N, and β-WC_{1-x} the non-metal sites are only partially occupied).

$$NH_3(g) \rightarrow {}^1/_2N_2(g) + {}^3/_2H_2(g) \quad (1)$$

$$NH_3(g) \rightarrow [N](s) + {}^3/_2H_2(g) \quad (2)$$

$$NH_3(g) \rightarrow {}^1/_2N_2(g) + 3[H](s) \quad (3)$$

Assuming (1) is kept from equilibrium, (2) and (3) will be in pseudo-equilibrium with the gas phase. Katsura[86] has shown that the activities of nitrogen and hydrogen can then be written as

$$a_N = \frac{1}{K_{P(NH_3)}} \frac{P_{NH_3}}{(P_{H_2})^{3/2}} \quad (4)$$

$$a_H = \sqrt[3]{\frac{1}{K_{P(NH_3)}} \frac{P_{NH_3}}{(P_{N_2})^{1/2}}} \quad (5)$$

Using the same method it can be shown that for C_2H_6/H_2 and CH_4/H_2 mixtures the carbon activities are given by eqs 6 and 7, respectively.

Table 5. Summary of the Materials Made via TPRe of Early Transition Metal Oxides

	carbide (CH_4)		nitride (NH_3)		two step		carbide (C_2H_6)	
precursor	final T (K)	S_g ($m^2\,g^{-1}$)	final T (K)	S_g ($m^2\,g^{-1}$)	final T (K)	S_g ($m^2\,g^{-1}$)	final T (K)	S_g ($m^2\,g^{-1}$)
MoO_3	1020	91	980	161	970	135	900	174
WO_3	1150	39	1050	67	1050	64	900	71
V_2O_5	1170	44	1073	51	1170	49	1023	76
H−Nb_2O_5	1170	62	973	82	1170	76	1023	113
L-Ta_2O_5	1220	54	1073	72	1170	70	no reaction	
$Mo_3Nb_2O_{14}$	1170	87	1073	68	1170	65	900	156
$W_9Nb_8O_{47}$	1170	88	1073	112	1170	107	900	102
$Mo_2Ta_2O_{11}$	1170	52	1123	59	1170	55	900	84

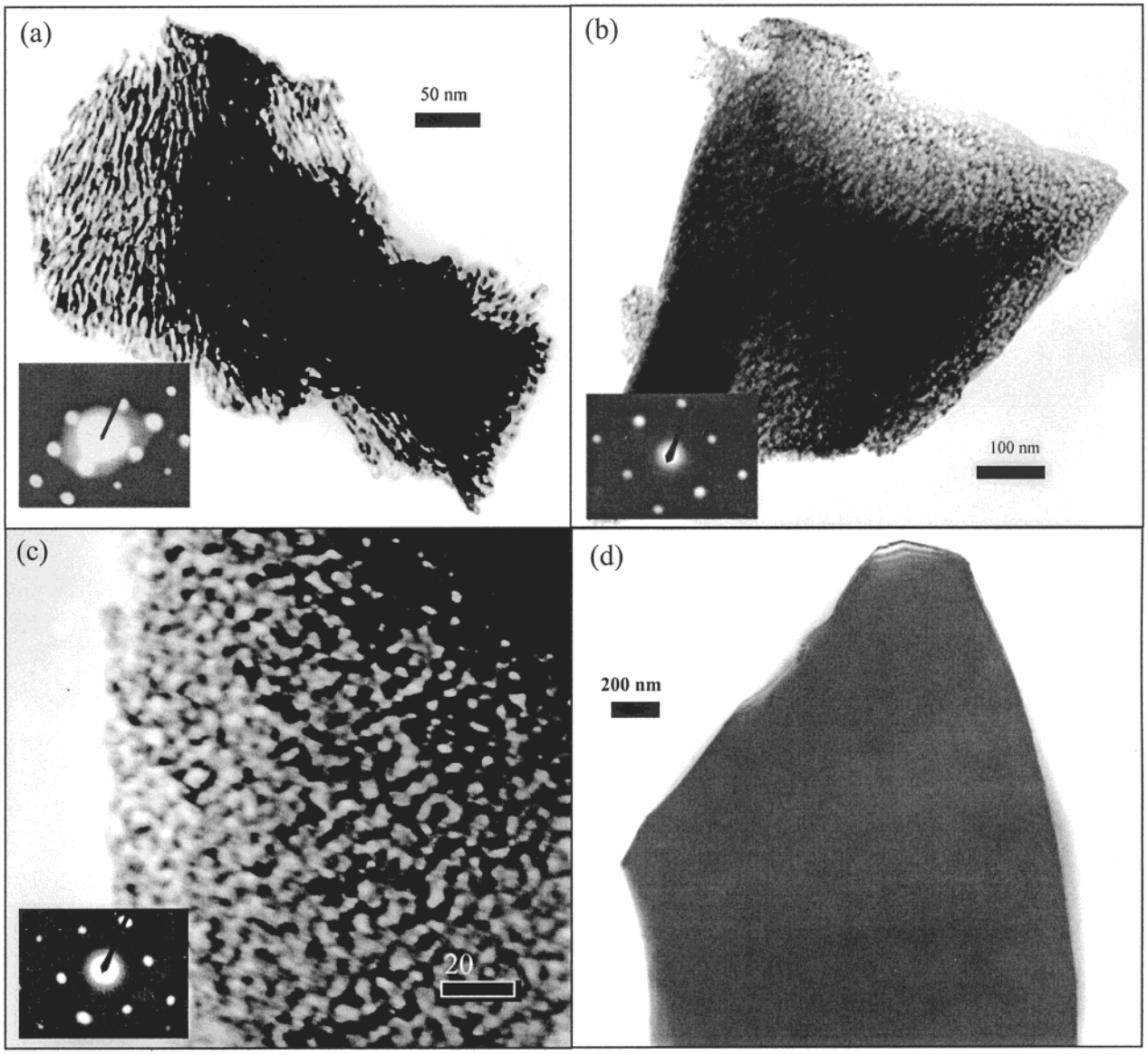

Figure 10. Micrograph showing a typical particle produced by the ammonia TPRe of ternary oxides. (a) Product of the TPRe of $WNb_{12}O_{33}$. The particle is made up of many smaller particles which, according to electron diffraction, are aligned. Note the appearance of fine fractures in the particle. (b) Product of the TPRe of $W_3Nb_{14}O_{44}$. The particle is made up of many smaller particles, which are shown to be aligned by electron diffraction. (c) Product of the TPRe of $W_9Nb_8O_{47}$. The particle is made up of smaller crystallites, which are shown to be aligned by SAED. (d) Pre-reaction $W_3Nb_{14}O_{44}$ particle for comparison.

$$a_C = \sqrt{\frac{1}{K_{P(C_2H_6)}}\frac{P_{C_2H_6}}{(P_{H_2})^3}} \tag{6}$$

$$a_C = \frac{1}{K_{P(CH_4)}}\frac{P_{CH_4}}{(P_{H_2})^2} \tag{7}$$

For oxides the situation is more complex, but for higher hydrocarbons we can still derive relationships between methane activities and gas composition, e.g. for ethane taking into account reaction 8.

$$C_2H_6(g) + H_2(g) \rightarrow 2CH_4(g) \tag{8}$$

$$a_{CH_4} = K_{P(CH_4)} \cdot \left(\sqrt{\frac{P_{C_2H_6}P_{H_2}}{K_{P(C_2H_6)}}}\right) \tag{9}$$

From the above, it can be seen that higher hydrocarbons should be promising reagents for the conversion

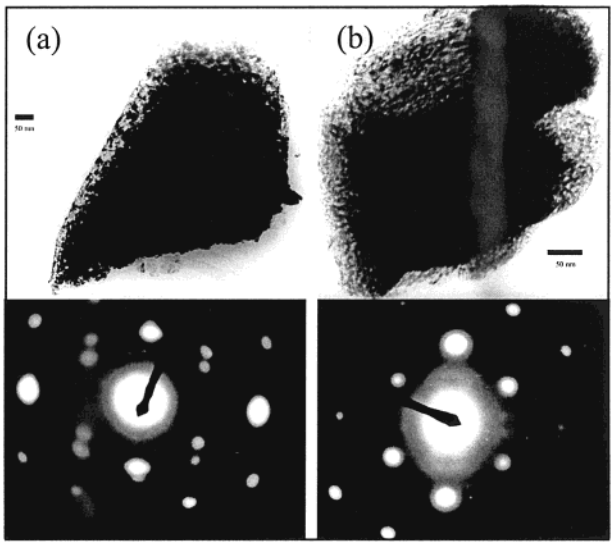

Figure 11. Micrographs showing typical particles produced by the temperature-programmed reaction of H−Nb_2O_5 by (a) ammonia and (b) ethane.

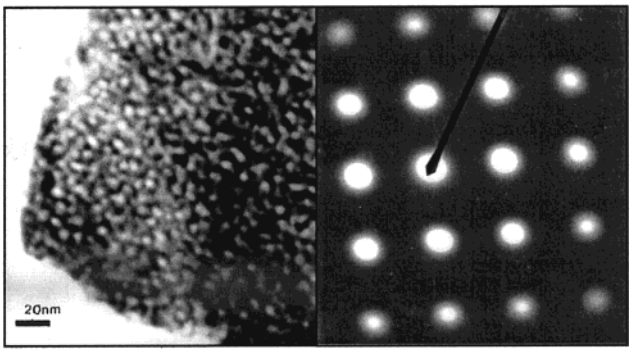

Figure 12. Micrograph of β-Mo_2C formed by the ethane TPRe of MoO_3 and electron diffraction showing $(2\bar{1}\bar{1}0)Mo_2C||(010)$-$MoO_3$.

of transition metal oxides to carbides under comparatively mild conditions, and indeed this is borne out by the results for the TPRe of the various oxides.

Comparison of the Available Routes. Table 5 summarizes the surface areas and synthesis temperatures employed in this study. Also included for comparison are some results obtained using previously described syntheses for molybdenum and tungsten systems.[48,49,68,91,92] There are several trends for the reactions, which can be seen to be general for binary and ternary oxides of group V and VI. In most cases, the use of the nitride as a precursor or ethane as a reactant increases the surface area of the products, as well as lowering the required synthesis temperature. Nitrides can be converted readily to the carbides while maintaining both the high surface area and structure of the nitride. Ethane TPRe gives materials with surface areas comparable to those of the two step oxide to nitride to carbide route, and in many cases the surface areas are higher, though it should be noted that the crystallinity of the materials prepared via the nitrides is superior. Also, as noted above, reaction temperatures for ethane are much lower than those for methane, as expected from the thermodynamics already discussed.

It is interesting that, for reactions with hydrocarbons, the presence of group VI metals enhances the rate of reaction, whereas for the reaction with ammonia they retard the reaction. The most probable explanation for this is that the group VI metals provide more easily reduced surface sites at which ammonia or hydrocarbons can dissociate; this effect has been demonstrated in the synthesis of Mo_2N[93,94] and VN.[71,95] In the case of the former, ammonia decomposition was near equilibrium, while in the latter much less than equilibrium ammonia decomposition is observed. In the case of ammonia, nitrogen is formed and lost to the gas phase. However, for hydrocarbons, the active species are trapped on the surface as highly reactive carbon species, since the activation barrier to the formation of bulk carbon is very high. The effect of promoting the reaction of hydrocarbons with oxides has been previously shown by Lee et al.[92] using Pt-promoted MoO_3. It should be noted that where several different phases can be formed, the choice of route can allow the synthesis of comparable surface area systems, e.g. β-Mo_2C and α-MoC_{1-x} and the various tungsten phases (see Figure 9). The reason for the inertness of L-Ta_2O_5 to ethane is unclear, though one possible explanation is that, as the initial reduction

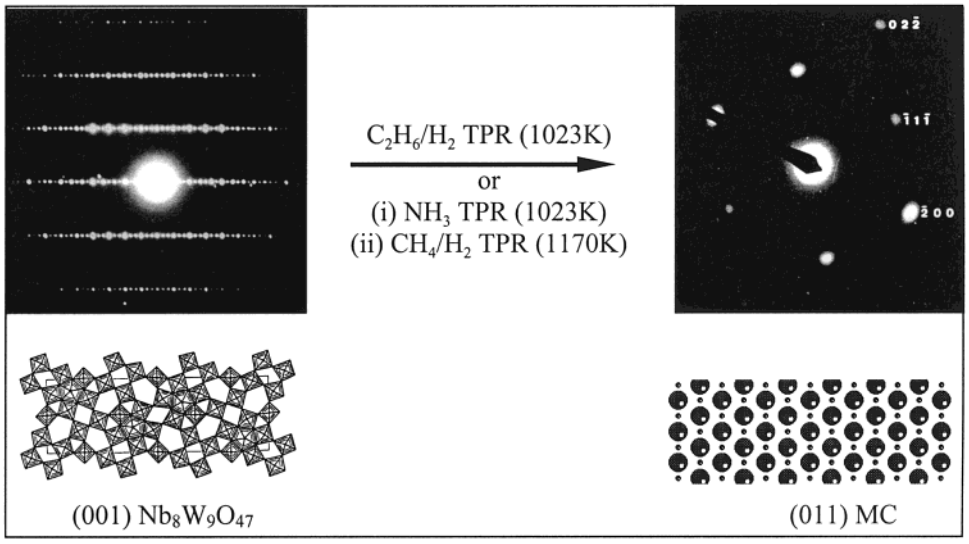

Figure 13. Representative selected area diffraction of $W_9Nb_8O_{47}$, and the products of ammonia and ethane TPRe with a tentative interpretation in terms of the structural relationship between the oxide and carbide (results for the nitridation were analogous).

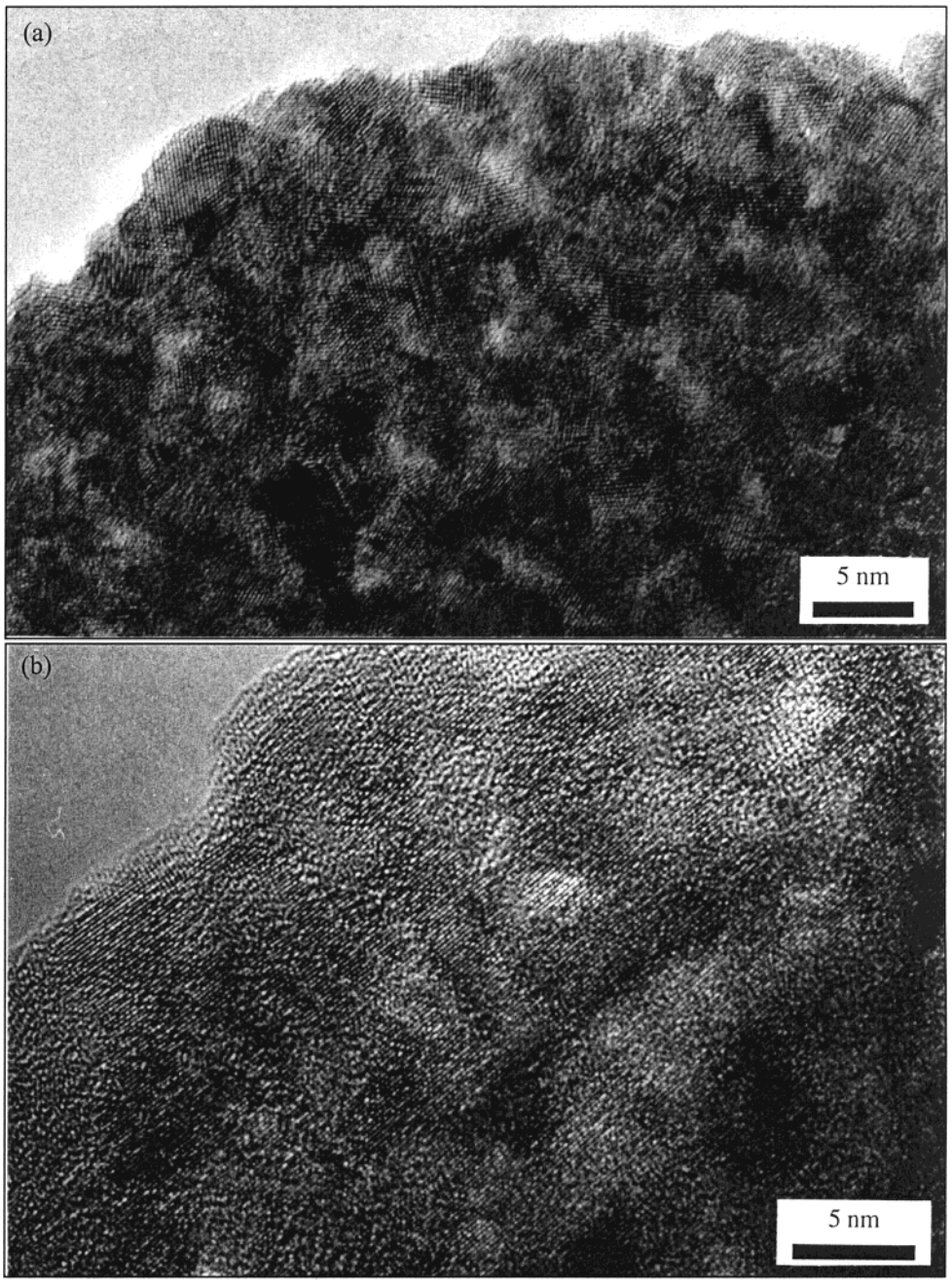

Figure 14. Representative high-resolution micrographs of the products of the TPRe: (a) the $W_9Nb_8C_x$ product of ethane TPRe; (b) NbN_x produced by ammonia TPRe.

of L-Ta_2O_5 is difficult, surface carbon is formed thereby blocking the surface to further reaction.

Morphological Evidence for the Topotaxy of the Reactions. Previously it has been shown that the nitridation of MoO_3, WO_3,[49] and V_2O_5,[95] together with the carburization of Mo_2N and W_2N,[48] proceeds topotactically, while the reactions of methane with Nb_2O_5[70] and V_2O_5[71] proceed pseudomorphically but not topotactically, and the reaction of methane[68,96] or synthesis gas[96] and forming gas[96] with MoO_3 does not proceed pseudomorphically. In other reported syntheses, no study of the relationships of the product and starting material was undertaken.

Before proceeding with a discussion of the nature of the reactions studied, it is first necessary to define the terms topotactic and pseudomorphic. Pseudomorphic is taken to mean that the overall morphology of the particles of starting material are maintained. The following is the generally accepted definition for topotactic:

"A process is called Topotactic if its solid product is formed in one or several crystallographically equivalent orientations as a consequence of chemical reaction or a solid-state transformation, and if it can proceed throughout the entire volume of the parent crystal."[97]

(91) Ribeiro, F. H.; Dalla Betta, R. A.; Guskey, G. J.; Boudart, M. *Chem. Mater.* **1991**, *3*, 805.
(92) Lee, J. S.; Volpe, L.; Ribeiro, F. H.; Boudart, M. *J. Catal.* **1988**, *112*, 44.
(93) Wise, R. S.; Markel, E. J. *J. Catal.* **1994**, *145*, 335.
(94) Wise, R. S.; Markel, E. J. *J. Catal.* **1994**, *145*, 344.
(95) Oyama, S. T. *Catal. Today* **1992**, *15*, 179.
(96) Li, S. Z.; Kim, W. B.; Lee, J. S. *Chem. Mater.* **1998**, *10*, 1853.

This means that if a reaction is topotactic it must proceed through each step maintaining information on the orientation of the starting material; for example, if an intercalation reaction proceeds via the exfoliation of the layers of the host, the reaction is not topotactic, despite the apparent relationship between the starting material and the product. It is, therefore, hard to unambiguously demonstrate the topotactic nature of a reaction, without continuously monitoring the reaction. However, the maintenance of a strong orientation effect does provide evidence of the topotactic nature of the reaction.[49,97] The nature of the products of the TPRe reactions were, therefore, studied by HRTEM. Typical micrographs are shown in Figures 10−12.

In all cases, the particles were made up of aggregates of smaller particles, which were on the order of magnitude indicated by BET and XRD measurements. All the materials maintained the gross morphology of the parent oxides, and this is clearly visible in Figure 10, where the irregular sharp sided morphology of the parent oxide is still clearly discernible. The particles are polycrystalline, and thus, electron diffraction would be expected to produce a ring pattern. Indeed, this is the case for the products of the TPRe of the oxides in methane.

However, in the case of TPRe with ammonia or ethane and the carburization of the nitrides, electron diffraction patterns consisting of spots indexable on a single orientation of the material were observed (Figures 10−12). This shows that the individual crystallites are all individually oriented along a crystallographically identical direction, giving strong evidence for the topotactic nature of the reaction.

For molybdenum oxide, the relationship between the oxide and carbide formed via the reaction with ethane can be easily obtained, as MoO_3 exhibits a strong tendency to form plates with (010) perpendicular to the plate. Thus, using electron diffraction it was possible to show that the β-Mo_2C was formed with $(2\bar{1}\bar{1}0)$ perpendicular to the plate, i.e., parallel to the (010) of the original MoO_3 (Figure 12). For the other oxides, no such preferred orientation is observed; however, the measurement of many electron diffraction patterns on crystallites of $W_9Nb_8O_{47}$ showed that, though not as pronounced as for MoO_3, most particles were oriented close to perpendicular to (001) and that most carbide and nitride particles were oriented perpendicular to (110) (Figure 13), leading to a probable transformation maintaining $W_9Nb_8O_{47}(001)||(110)W_9Nb_8N_x/W_9Nb_8C_x$.

Figure 14 shows higher magnification HRTEM images of $W_9Nb_8C_x$ and NbN_x. In all cases, the variable thickness of the sample can be seen as a mottling of the particle, and lattice fringes can be seen extending over distances considerably larger than the crystallites, again showing the orientational relationship between the individual crystallites.

Conclusions

Boudart's TPRe method has been further investigated and appears to be a versatile method for producing high surface area early transition metal nitrides and carbides. Both low surface area oxides and high surface area nitrides can be used as precursors, and binary and ternary systems can be synthesized using methane, ethane, or ammonia as reactants. Reactions of ethane and ammonia with the precursor oxides appear to proceed topotactically.

Ethane reactions tend to proceed at lower temperatures than either ammonia or methane. For reactions with ethane or methane the reaction temperatures required for conversion of ternary niobium and tantalum oxides are lower than for niobia and tantalia, however with ammonia higher final temperatures are required.

Further work on the synthesis of supported systems and those containing different metals would be worthwhile and work is continuing to explore the catalytic properties of the materials.

Acknowledgment. The authors wish to thank Dr. Jeremy Sloan for his help with the electron microscopy. J.B.C. wishes to thank British Gas plc for a CASE award, and A.J.B. is grateful to the Rhodes trust for a Rhodes Scholarship.

CM9911060

(97) Oswald, H. R.; Günter, J. R. *Crystal Growth and Materials*; North-Holland: Amsterdam, 1977.